Cent. Eur. J. Chem. • 7(3) • 2009 • 439-445
DOI: 10.2478/s11532-009-0033-z

VERSITA

Central European Journal of **Chemistry**

QSPR study for the prediction of half-wave potentials of benzoxazines by heuristic method and radial basis function neural network

Research Article

Huitao Liu[1*], Yingying Wen[1], Feng Luan[1], Yuan Gao[1], Xiuyong Li[2]

[1] *Department of Applied Chemistry,*
Yantai University,
Yantai 264005, P. R. China

[2] *Yantai Inspection and Quarantine Bureau,*
Yantai 264000, P. R. China

Received 20 November 2008; Accepted 03 January 2009

Abstract: The half-wave potential ($E_{1/2}$) is an important electrochemical property of organic compounds. In this work, a quantitative structure–property relationship (QSPR) analysis has been conducted on the half-wave reduction potential ($E_{1/2}$) of 40 substituted benzoxazines by means of both a heuristic method (HM) and a non-linear radial basis function neural network (RBFNN) modeling method. The statistical parameters provided by the HM model ($R^2 = 0.946$; $F=152.576$; $RMSCV=0.0141$) and the RBFNN model ($R^2=0.982$; $F=1034.171$ and $RMS = 0.0209$) indicated satisfactory stability and predictive ability. The obtained models showed that benzoxazines with larger Min valency of a S atom (MVSA), lower Relative number of H atom (RNHA) and Min n-n repulsion for a C-H bond (MnnRCHB) and Minimal Electrophilic Reactivity Index for a C atom (MERICA) can be more easily reduced . This QSPR approach can contribute to a better understanding of structural factors of the organic compounds that contribute to the $E_{1/2}$, and can be useful in predicting the $E_{1/2}$ of other compounds.

Keywords: *Heuristic method • Radial basis function neural network (RBFNN) • Quantitative structure–property relationship (QSPR) • Half-wave potential • Benzoxazine*

1. Introduction

With the development of synthetic chemistry, a large number of new compounds are synthesized every year. Physicochemical properties, biological activities and other properties of these compounds are required to be determined. So far, there are many methods to investigate the properties mentioned above. However, many of these compounds are not tested for fundamental or relevant thermodynamic and physicochemical properties or biological activities, which still remain unknown due to unavailability or handling difficulties (toxicity, odor, instability, solubility *etc.*).

At the present time, quantitative structure–property relationships (QSPR) are increasingly employed in the prediction of chemical and physical properties of different types of molecules [1-8]. The main task of QSPR is to obtain a reliable model for the prediction of properties/behaviors of new chemical substances and analytical systems. These relationships derive correlations between the structural similarities of individual compounds and their biological activity/chemical properties.

The half-wave potential ($E_{1/2}$), which is an important electrochemical property for a reversible oxidation–reduction system, can be useful for predicting other electrochemical properties and activities of organic compounds. In the reduction of many organic compounds, the reaction is a one-electron process that produces a radical anion, $Q^{\bullet-}$, according to the following equation:

$$Q + e = Q^{\bullet-} \tag{1}$$

However, because $Q^{\bullet-}$ is generally reactive, its lifetime varies over a wide range, depending on its intrinsic reactivity and experimental conditions, such as the type of solvent, complex formation, and other chemical reactions [9]. Nesmerak *et al.* have demonstrated a

---

* *E-mail: liuht@lzu.edu.cn*

QSPR method for the prediction of $E_{1/2}$ of benzoxazines [10]. In [10] the correlation equation was developed using Hammett constants of substituents and type of heteroatom as the descriptors. Another equation was proposed using half-wave potential *vs.* energy of highest-occupied molecular orbital. However the R^2 values of the two models were 0.823 and 0.897 respectively, which are smaller than that obtained with our models. And in [10] only linear model was used. Yuan *et al*. developed a QSPR method for the half-wave potential of substituted phenols using a support vector machine (SVM). Nikolic *et al*. reported a QSPR analysis of the $E_{1/2}$ of 36 benzenoid hydrocarbons. Fatemi *et al*. used a QSPR method to predict the effect of different solvents on the $E_{1/2}$ [7-9]. Multiple linear regression (MLR) was used to develop a QSPR model to predict the reduction $E_{1/2}$ values for nitrobenzene derivatives in five different solvents. Results showed that the QSPR method using MLR can generate suitable models for the prediction of reduction $E_{1/2}$ values for these compounds using electronic descriptors for solutes and solvents.

Benzoxazines are bicyclic heterocyclic compounds, which are commonly prepared by a Mannich-like condensation of phenol, formaldehyde and an amine. From the pharmaceutical point of view, benzoxazine derivatives possess bacteriostatic, and immunomodulating activity, and have been used as neuroprotective antioxidants, *etc* [10].

In this work, two QSPR methods, an heuristic method (HM) and a radial basis function neural network (RBFNN), were used to predict the $E_{1/2}$ of some benzoxazines, and the results of the prediction were satisfactory. Moreover, according to our best knowledge, no QSPR study using RBFNN for the prediction of the $E_{1/2}$ of organic compounds has been reported yet.

2. Experimental Procedures

2.1. Data set

A database of 40 substituted benzoxazines (see Fig. 1 for the general structure and Table 1 for the substituents) and the values of their $E_{1/2}$s were taken from literature [11].

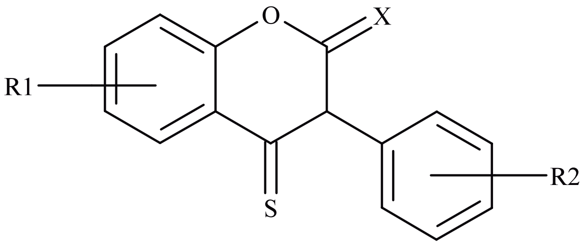

Figure 1. General structure of the compounds

2.2. Descriptor calculation

The three-dimensional structures of the substituted benzoxazines were drawn using the Hyperchem [12]. The Hyperchem program was used to generate the preliminary molecular geometry optimization using molecular mechanics MM+ force fields [13]. The final optimization was obtained using the semiempirical PM3 [14] parametrization method present in the MOPAC computer program [15]. Then the structural files were transferred into CODESSA software for producing descriptors [16,17]. In this work, 562 total constitutional, topological, geometrical, electrostatic and quantum-chemical descriptors were calculated.

2.3. Heuristic method

Whether the QSPR model is successful or not is largely determined by the selection of descriptors, and their ability to represent the essential determinants of the molecular properties. There are many classification methods for screening of the descriptor pool, such as an HM [1], cluster analysis [18], neural net classification [19], genetic algorithm [20], *etc*. In the present study, an HM method was used to select the descriptors, and to develop a linear model for the prediction of $E_{1/2}$. The HM in CODESSA was employed to select the suitable descriptor combinations to build the linear QSPR models [21]. The HM of the descriptor selection proceeds with a preselection by eliminating descriptors that (i) are not available for each structure; (ii) have a small variation in magnitude for all structures; (iii) have a Fisher F-criterion below 1.0; and (iv) have *t*-values less than the user-specified value (by default 0.1), *etc*.

The next step involves correlation of the given property with (i) the top descriptor in the above list with each of the remaining descriptors and (ii) the next one with each of the remaining descriptors, *etc*. Thus, MLR models are developed in a stepwise procedure and correlations are ranked according to the values of the correlation coefficient (R^2) and the F-criterion. Starting with the top descriptor from the list, two-parameter correlations are calculated. In the following steps new descriptors are added one-by-one until the pre-selected number of descriptors in the model is achieved. The final result is a list of the 10 best models according to the values of the F-test and correlation coefficient. The fit of the model is tested by the coefficient of determination (R^2), the F-test (F) and the standard deviation (s^2) [22].

2.4. Radial basis function neural networks

A radial basis function neural network was also constructed to model the structure property relationship. The theory of different networks has been extensively

Table 1. Structures, experimental and predicted $E_{1/2}$ for the compounds

No.	X	R1	R2	Experimental	Predicted	
				$E_{1/2}$(V)	$E_{1/2(HM)}$(V)	$E_{1/2(RBFNN)}$(V)
1	O	7-OCH_3		1.420	1.402	1.421
2	O	7-OCH_3	4-F	1.430	1.437	1.426
3	O	7-OCH_3	4-Br	1.440	1.456	1.447
4	O	7-OCH_3	3-F	1.445	1.462	1.436
5	O	7-OCH_3	3-Cl	1.450	1.462	1.455
6	O	7-CH_3	4-CH_3	1.415	1.385	1.419
7	O	6-CH_3	4-CH_3	1.420	1.425	1.421
8	O		4-Br	1.490	1.495	1.491
9	O	6-OCH_3	4-CH_3	1.450	1.432	1.446
10	O	6-OCH_3	4-F	1.460	1.451	1.462
11	O	6-OCH_3	4-Br	1.465	1.495	1.491
12	O	6-OCH_3	4-Cl	1.470	1.470	1.463
13	O	6-OCH_3	3-F	1.480	1.483	1.479
14	O	6-OCH_3	4-CN	1.510	1.514	1.495
15	O	6-Cl		1.530	1.533	1.529
16	O	6-Cl	3-Cl	1.590	1.569	1.593
17	S	7-OCH_3	4-CH_3	1.280	1.288	1.277
18	S	7-OCH_3		1.315	1.332	1.322
19	S	7-OCH_3	4-F	1.350	1.364	1.351
20	S	7-OCH_3	4-Br	1.360	1.375	1.369
21	S	7-OCH_3	4-Cl	1.370	1.369	1.364
22	S	7-OCH_3	3-F	1.390	1.385	1.384
23	S	7-OCH_3	3-Cl	1.395	1.375	1.370
24	S	7-OCH_3	4-CF_3	1.405	1.414	1.430
25	S	7-OCH_3	3,4-Cl_2	1.420	1.402	1.420
26	S	7-CH_3	4-CH_3	1.305	1.295	1.316
27	S	6-CH_3	4-CH_3	1.320	1.321	1.326
28	S		4-Br	1.420	1.417	1.420
29	S	6-OCH_3	4-CH_3	1.330	1.338	1.322
30	S	6-OCH_3		1.360	1.364	1.368
31	S	6-OCH_3	4-F	1.380	1.399	1.402
32	S	6-OCH_3	4-Br	1.400	1.400	1.393
33	S	6-OCH_3	4-Cl	1.400	1.399	1.402
34	S	6-OCH_3	3-F	1.410	1.409	1.416
35	S	6-OCH_3	3-Cl	1.430	1.405	1.411
36	S	6-OCH_3	4-CF_3	1.440	1.449	1.452
37	S	6-OCH_3	3,4-Cl_2	1.445	1.443	1.444
38	S	6-OCH_3	4-CN	1.450	1.423	1.433
39	S	6-Cl		1.420	1.447	1.454
40	S	6-Cl	3-Cl	1.520	1.497	1.499

presented in several papers [23,24]. Here is a brief description of the RBFNN principle. Fig. 2 shows the basic network architecture. It consists of an input layer, a hidden layer, and an output layer. The input layer does not process the information; it only distributes the input vector to the hidden layer. The hidden layer of RBFNN consists of a number of radial basis function (RBF) units (n_h) and bias (b_k). Each hidden layer unit represents a single RBF, with associated center position and width. Each neuron on the hidden layer employs an RBF as a nonlinear transfer function to operate on the input data. The most often used RBF is a Gaussian function that is characterized by a center (c_j) and a width (r_j). The RBF measures the Euclidean distance between the input vector (X) and the RBF center (c_j) and performs the non-linear transformation with the RBF in the hidden layer as given below:

$$h_j(X) = exp\left(-\left\|X - c_j\right\|^2 / r_j^2\right) \qquad (2)$$

In which h_j is the notation for the output of the j_{th} RBF unit. For the j_{th} RBF, c_j and r_j are the center and the width, respectively. The operation of the output layer is linear, which is given below:

$$y_k(X) = \sum_{j=1}^{n_k} w_{kj} h_j(X) + b_k \tag{3}$$

Where y_k is the k_{th} output unit for the input vector X, w_{kj} is the weight connection between the k_{th} output unit and the j_{th} hidden layer unit, and b_k is the bias. It can be seen from Eqs. (2) and (3), a RBFNN involves selecting the center, number of hidden layer units, width, and weights. There are various ways for selecting the center, such as random subset selection, K-means clustering, orthogonal least squares learning algorithm, RBF-PLS (radial basis function - partial least squares), *etc*. The widths of the RBF networks can either be chosen the same for all the units or can be chosen differently for each unit. In this paper, considerations were limited to Gaussian functions with a constant width, which was the same for all units. The adjustment of the connection weight between hidden layer and output layer is performed using a least-squares solution after the selection of the centers and widths of the RBFs.

The overall performance of the RBFNN is evaluated in terms of a root-mean-squared error (RMS) according to the equation below:

$$RMS = \sqrt{\frac{\sum_{i=1}^{n_k} \left(y_k - y_{k,0}\right)^2}{n_k}} \tag{4}$$

Where y_k is the desired output and $y_{k,0}$ is the actual output of the network; n_k is the number of compounds in analyzed set. The performance of RBFNN is determined by the values of following parameter: The number n_h of radial basis functions, the center c_j and the width r_j of each radial basis function, the connection weight w_{kj} between the j_{th} hidden layer unit and the k_{th} output unit. The center of the RBFNN is determined with the forward subset selection method proposed by Orr [25,26]. The optimal width was determined by experiments with a number of trials by taking into account the leave-one-out (LOO) cross-validation error. The one that gives a minimum LOO cross-validation error is chosen as the optimal value.

All calculation programs implementing the RBFNN were written in M-file based on a MATLAB script for RBFNN [25,26]. The RBFNN toolbox in MATLAB 7.0 was used to develop this RBFNN. The scripts were run on a Personal Computer.

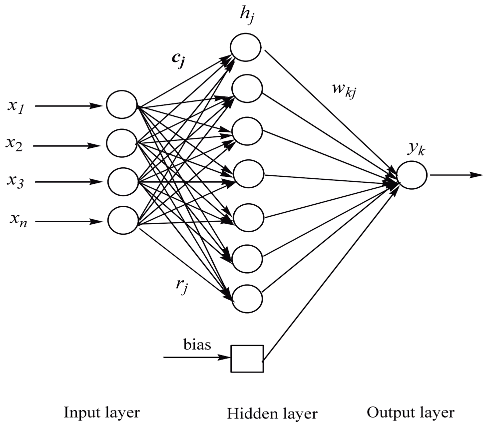

Figure 2. The architecture of RBFNN

3. Results and discussion

3.1. Results of the HM

The HM was used to develop a linear model for the prediction of $E_{1/2}$ using calculated structural descriptors. After the heuristic reduction, the pool of descriptors was reduced from 562 to 173. Good correlations with the experimental $E_{1/2}$ data were selected based on the squared correlation coefficient (R^2), F-criterion (F), root-mean-squared error of cross validation (RMSECV) and Q^2 of the regression. After the heuristic reduction, ten best models with four descriptors were selected. Then, the model with the highest R^2 was chosen for analysis. The multi-linear analysis of $E_{1/2}$ values for the 40 compounds produced a four-parameter model. The obtained descriptors, coefficients, standard errors and *t*-test statistic are summarized in Table 2. In addition, the plot of predicted and experimental values is shown in Fig. 3.

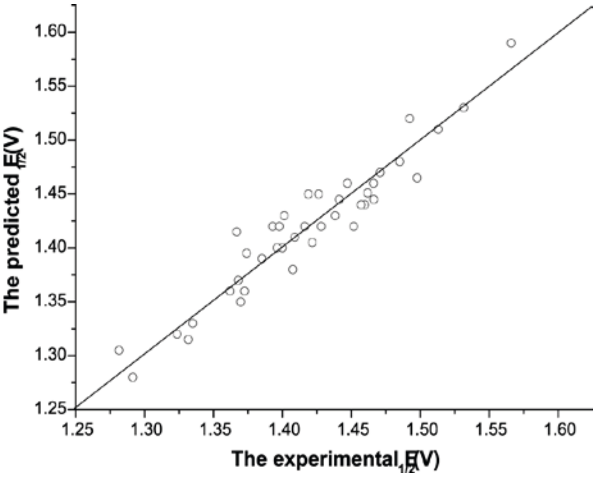

Figure 3. Experimental $E_{1/2}$ versus predicted $E_{1/2}$ by HM

Table 2. Descriptors, Coefficients, Standard Error, and t-Test Values for the HM model

Descriptors	Coefficients	Standard Error	t-test
Intercept	2.026e+01	5.574e+00	3.635
Min valency of a S atom	4.457e+00	3.600e-01	12.382
Relative number of H atoms	-9.612e-01	7.489e-02	-12.834
Min n-n repulsion for a C-H bond	-6.768e-01	1.344e-01	-5.034
Min electrophilic reactivity Index for a C atom	-1.760e+04	4.989e+03	-3.528

R^2 =0.946; F=152.576; R^2_{cv}=0.927; RMSCV=0.0141; Q^2=0.946

Table 3. Validation of correlations for the HM and RBFNN models

		HM						RBFNN					
		For the training set			For the test set			For the training set			For the test set		
Training set	Test set	R^2	RMSCV	F	R^2	RMS	F	R^2	RMS	F	R^2	RMS	F
A+B+C+D	E	0.949	0.0141	125.710	0.930	0.0179	79.149	0.913	0.0192	970.266	0.862	0.162	37.447
A+B+C+E	D	0.952	0.0141	134.480	0.910	0.0184	60.346	0.992	0.00850	1736.100	0.592	0.0343	8.703
A+B+D+E	C	0.951	0.0173	130.603	0.907	0.0163	58.428	0.991	0.00870	1658.584	0.832	0.0227	29.746
A+B+D+E	B	0.932	0.0173	92.913	0.992	0.00630	749.212	0.976	0.0137	589.340	0.977	0.0153	251.500
B+C+D+E	A	0.961	0.0141	167.740	0.887	0.0274	47.104	0.982	0.0112	970.266	0.862	0.0386	37.543

From Table 2 we can see that four descriptors have the major effect on $E_{1/2}$. Among them, only Min valency of a S atom (MVSA) has a positive effect on the $E_{1/2}$ value, which means that the $E_{1/2}$ value will increase with the MVSA. While the other three descriptors, Relative number of H atoms (RNHA), Min n-n repulsion for a C-H bond (MnnRCHB) and Min electrophilic reactivity Index for a C atom (MERICA), have negative effects on the $E_{1/2}$ value.

To demonstrate the absence of chance correlations, the internal validation method was used. A fivefold cross-validation algorithm was applied for validation of the prediction results. In this process, the whole data set was split into five equally sized parts: A (1,6,11, ..., 36), B (2,7,12, ..., 37), C (3,8,13, ..., 38), D (4,9,14, ..., 39) and E (5, 10, 15, …, 40). Each subset was predicted by using the other four subsets as the training set. For each training set, the correlation equation was derived with the same descriptors, and the equation obtained was used to predict $E_{1/2}$ values for the compounds from the corresponding test set. The reported R^2, F and RMS for each cross-correlation are shown in Table 3. From the table we can see that the values were similar. We therefore concluded that the final model is considered to be stable.

3.2. Results of RBFNN

Using the four molecular descriptors, a RBFNN non-linear model was developed. Such a RBFNN can be designed as 4-n_k-1 net to indicate the number of units in the input, the hidden layer and output layer, respectively. To obtain better results, the parameter that influenced the performance of RBFNN was optimized. The selection of the optimal width value for RBFNN was performed by systemically changing its value in the training step. The value that gives the best leave one out (LOO) cross-validation result was used in the model. Based on the above optimization, the value of the optimal width is 3.1 and the corresponding number of centers (hidden layer nodes) of RBFNN is 18. The plot of predicted and experimental values for the RBFNN method is shown in Fig. 4. The R^2, F and RMS are 0.982, 1034.171 and 0.0209, respectively.

In addition, a fivefold cross-validation algorithm, like that described above for the HM, was applied to validate further the predictions of the non-linear model. The R^2, F and RMS of each cross-correlation are also listed in Table 3.

From Table 3, we can see that the performances of the model developed by RBFNN are similar to those developed by HM. The only exception is that when using part D as the test set, the performance of the RBFNN was relatively poorer than the others, indicating that the non-linear model developed is a little bit less stable than the linear one. And from Figs. 3 and 4, we can see that both methods satisfactorily predict the experimental $E_{1/2}$. Comparative residuals *vs.* compounds for the HM and RBFNN models are shown in Fig. 5. Both the HM and RBFNN models resulted in satisfactorily small residuals (relative error <1.6%).

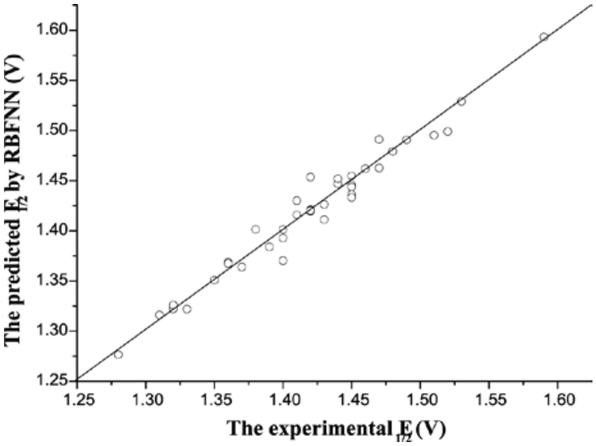

Figure 4. Experimental $E_{1/2}$ versus predicted $E_{1/2}$ by RBFNN

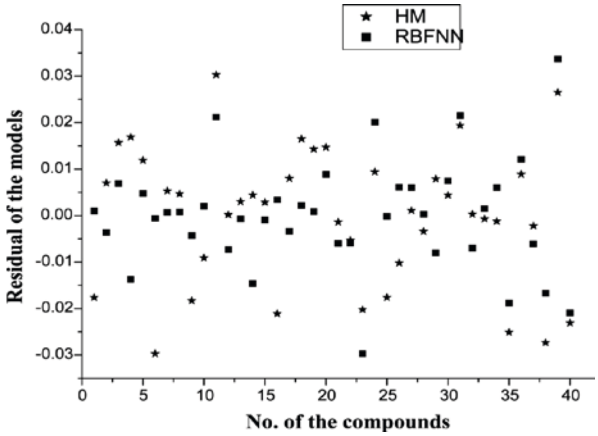

Figure 5. Plot of residual vs. No. of the compounds by HM and RBFNN

3.3. Discussions of the input parameters

By interpreting the descriptors in the model, it is possible to gain some insight into the factors affecting the half-wave potential value and understand which interactions play an important role during the reduction reaction. In the linear model, four descriptors were found to be important for these compounds.

RNHA is a constitutional descriptor reflecting only the molecular composition of the compound without using the geometry or electronic structure of the molecule. The negative coefficient of RNHA means that the greater the number of H atoms in the molecule, the more difficult it is for the molecule to accept an electron, leading to a more negative $E_{1/2}$ value.

MVSA, MnnRCHB and MERICA are three quantum-chemical descriptors. Changing the substitution can cause a change in polarization and electron density around the ring in both reactant and product. It is apparent from the experimental data that the $E_{1/2}$ value of each benzoxazine is affected by the type of substitution on the benzene ring. Substitutions with a higher valency can easily accept an electron; therefore, an increase in MVSA causes an increase in $E_{1/2}$.

MnnRCHB describes the nuclear repulsion driven processes in the molecule and may be related to the conformational (rotational, inversional) changes or atomic reactivity in the molecule [27]. If the descriptor is lower, the compound is more stable making the reduction more difficult and which results in smaller $E_{1/2}$ values. Consequently, MnnRCHB has a negative effect on $E_{1/2.}$

MERICA is a kind of charge distribution-related descriptor. The reactivity indices estimate the relative reactivity of the atoms in the molecule for a given series of compounds and are related to the activation energy of the corresponding chemical reaction. The negative coefficient of MERICA indicates that in the reduction reactions, the larger the MERICA, the more unfavorable it is for the compound to accept an electron, and the $E_{1/2}$ value will be smaller.

4. Conclusion

The present study demonstrates that both linear and nonlinear QSPR models based on descriptors calculated from the molecular structures of a set of 40 benzoxazines can be used for the successful prediction of half-wave potentials. The high R^2 and low RMS values obtained from the models suggest that both of the models have good predictive ability. Therefore the HM method and RBFNN can be used independently to predict the half-wave potential with satisfactory results.

Acknowledgment

We are grateful for financial support from the Foundation of Shandong Provincial Educational Department (J04D01) and the postdoctoral foundation of Yantai University (HY03B12).

References

[1] B.B. Xia, W.P. Ma, B. Zheng, X.Y. Zhang, B.T. Fan, Eur. J. Med. Chem. 43, 1489 (2008)

[2] J. Ghasemi, S. Saaidpour, J. Inclusion Phenom. Macrocyclic Chem. 60, 339 (2008)

[3] S.S. Godavarthy, R.L. Robinson, K.A.M. Gasem, Fluid Phase Equilib. 264, 122 (2008)

[4] A.R. Katritzky, I.B. Stoyanova-Slavova, D.A. Dobchev, M. Karelson, J. Mol. Graphics Modell. 26, 529 (2007)

[5] B. Hemmateenejad, M. Shamsipur, Internet Electronic J. Mol. Des. 2, 1 (2003)

[6] M. Shamsipur, A. Siroueinejad, B. Hemmateenejad, A. Abbaspour, H. Sharghi, K. Alizadeh, S. Arshadi, J. Electroanal. Chem. 600, 345 (2007)

[7] S. Yuan, M. Xiao, G. Zheng, M. Tian, X. Lu, SAR QSAR Environ. Res. 17, 473 (2006)

[8] S. Nikolic, A. Milicevic, N. Trinajstic, Croat. Chem. Acta 79, 155 (2006)

[9] M.H. Fatemi, M.R. Hadjmohammadi, K. Kamel, P. Biparva, Bull. Chem. Soc. Jpn. 80, 303 (2007)

[10] K. Nesmerak, I. Nemec, M. Sticha, K. Waisser, K. Palat. Electrochim. Acta 50, 1431 (2005)

[11] A. Toropov, K. Nesmerak, I. Ralka, K. Waisser, K. Palat, Comput. Biol. Chem. 30, 434 (2006)

[12] HyperChem 4.0, Hypercube Inc., Gainesville, FL, 1994

[13] HyperChem 6.01, Hypercube, Inc., 2000

[14] M.J.S. Dewar, E.G. Zoebisch, E.F. Healy, J.J.P. Stewart, J. Am. Chem. Soc. 107, 3898 (1985)

[15] J.J.P. Stewart, MOPAC, v.6.0 Quantum Chemistry Program Exchange, Program 455 (Indiana University, Bloomington, IN, 1989)

[16] A.R. Katritzky, V.S. Lobanov, M. Karelson, CODESSA: Training Manual (University of Florida, Gainesville, FL, 1995)

[17] A.R. Katritzky, V.S. Lobanov, M. Karelson, CODESSA: Reference Manual (University of Florida, Gainesville, FL, 1994)

[18] S.C. Basak, B.D. Gute, A.T. Balaban, Croat. Chem. Acta, 77, 331 (2004)

[19] J.V. Turner, D.J. Cutler, I. Spence, D.J. Maddalena, J. Comput. Chem. Jpn. 24, 891 (2003)

[20] F. Gharagheizi, Computational Materials Science 40, 159 (2007)

[21] M. Oblak, M. Randic, T. Solmajer, J. Chem. Inf. Comput. Sci. 40, 994 (2000)

[22] W.P. Ma, F. Luan, H.X. Zhang, X.Y. Zhang, M.C. Liu, Z.D. Hu, B.T. Fan, Analyst 131, 1254 (2006)

[23] X.J. Yao, A. Panaye, P. Doucet, R.S. Zhang, H.F. Chen, M.C. Liu, Z.D. Hu, B.T. Fan, J. Chem. Inf. Comput. Sci. 44, 1257 (2004)

[24] Y.H. Xiang, M.C. Liu, X.Y. Zhang, R.S. Zhang, Z.D. Hu, B.T. Fan, D.J.P. Panaye, J. Chem. Inf. Comput. Sci. 42, 592 (2002)

[25] M.J.L. Orr, Introduction to Radial Basis Function Networks (Centre for Cognitive Science, Edinburgh University, Scotland, 1996) http://www.anc.ed.ac.uk/~mjo/rbf.html (12/06/2001)

[26] M.J.L. Orr, MATLAB routines for subset selection and ridge regression in linear neural networks (Centre for Cognitive Science, Edinburgh University, Scotland, 1996) http://www.anc.ed.ac.uk/~mjo/rbf.html (12/06/2001)

[27] A.T. Balaban, S.C. Basak, A. Beteringhe, D. Mills, C.T. Supuran, Mol. Divers. 8, 401 (2004)